**Solid Freeform Fabrication 2025: Proceedings of the 36th Annual International
Solid Freeform Fabrication Symposium – An Additive Manufacturing Conference
Reviewed Paper**

Microstructure and Mechanical Properties of Bulk EB-PBF Fabricated Gamma-TiAl: Post-HIP and Heat Treatment Effects

S. T. Nabil*†, K. I. Watanabe*†, F. Medina*†

*Department of Aerospace and Mechanical Engineering, University of Texas at El Paso, El Paso, TX 79968

†W.M. Keck Center for 3D Innovation, University of Texas at El Paso, El Paso, TX, 79968

*Corresponding author (snabil@miners.utep.edu) at The University of Texas at El Paso

Abstract

Gamma Titanium aluminide (TiAl) is widely used in aerospace and defense for its high strength-to-weight ratio and creep resistance. GE implemented gamma-TiAl in their GEnx engine turbine, which significantly reduced fuel consumption, noise, and NOx emissions. However, the traditional processing of intermetallics, such as Ti-Al, remains challenging. Additive manufacturing techniques like electron beam powder bed fusion (EB-PBF) can offer an alternative. This study explores the fabrication of bulk TiAl rods using EB-PBF followed by hot isostatic pressing (HIP) and tailored heat treatments. Specimens underwent annealing with controlled cooling, aging, and quenching to refine the microstructure. Mechanical performance was evaluated through tensile tests according to ASTM E8 at ambient temperature and per ASTM E21-20 at elevated temperatures. Heat-treated EB-PBF TiAl exhibited markedly improved tensile properties, reduced anisotropy, and improved mechanical performance. These findings demonstrate the viability of combining EB-PBF, HIP, and optimized heat treatments to produce high-performance titanium aluminide for aerospace and defense applications.

Keywords
Electron Beam Powder-Bed Fusion (E-PBF), Titanium alloy, Hot Isostatic Pressing, Additive Manufacturing, Heat Treatment, Intermetallic

Introduction

Gamma Titanium aluminide (γ-TiAl) is an intermetallic alloy composed of almost an equal ratio of Titanium (Ti) and Aluminum (Al) [1]. This alloy is widely popular because it has a lower density ranging from 3.8 to 4.0 g/cm^3, which is almost half that of nickel-based superalloys (around 8 g/cm^3)[2], [3]. This enables it to have higher specific strength and remain stable at elevated temperatures, providing greater creep resistance up to 900 °C compared to Ni-based alloys, which can resist up to 650 °C, making it a good material for aerospace and aviation applications.[4], [5].

Due to this, γ-TiAl has been widely used in low-pressure turbine blades of General Electric's (GE) GEnx engine, which powers the Boeing 787 and 747 aircraft[6]. Implementing this material has enabled GE to reduce fuel consumption by up to 20%, decrease NOx emissions by 80%, and decrease noise by 50%[7], [8]. Additionally, this alloy has the potential for use in supersonic and hypersonic applications since it can be heated at around 1600°C on the leading edge[9]. In addition, it is nowadays used for turbocharger rotors and exhaust valves in the automotive industry[10].

γ-TiAl alloys consist of intermetallic compounds with long-range atomic ordering. The dominant gamma phase (γ) has a face-centered tetragonal structure and forms in compositions containing 49–66% aluminum[11], [12]. This phase exhibits high specific stiffness and oxidation resistance, but suffers from poor ductility at temperatures below 750 °C due to the limited availability of slip systems[13]. The α phase, characterized by a hexagonal close-packed structure and often coexisting with γ in a lamellar configuration, enhances both strength and brittleness [14], [15]. The β phase enhances hot workability and is stabilized by β-stabilizing elements such as Nb and Mo [16]. Upon cooling, it can transform into the ordered β_0 phase, which, although structurally stable, is brittle and known to serve as crack initiation sites [17]. In Nb-rich systems, the orthorhombic O-phase found in Ti_2AlNb alloys offers an alternative with superior room-temperature ductility and toughness.[18]

γ-TiAl alloys offer exceptionally high-temperature strength, but their ordered intermetallic nature poses significant challenges to conventional manufacturing[19]. The strong directional bonding and limited dislocation mobility result in poor ductility, especially at room temperature, with tensile elongations often below 2%[16].

Traditional methods such as casting and forging are similarly limited[20], [21]. In casting, the high reactivity of molten γ-TiAl with ceramic molds causes contamination and alpha-case formation, requiring expensive mold systems and leading to high defect rates[22]. Forging demands extremely narrow processing windows, high temperatures, and low strain rates, often resembling creep-forming rather than conventional deformation[4]. While β-stabilized variants like the TNM alloy have improved workability, processing remains complex and costly[23]. Fusion welding is also problematic due to cracking and the formation of brittle α_2-Ti_3Al in the heat-affected zones[14], [24].

To address the well-known challenges of manufacturing γ-TiAl using traditional methods, this study explores the use of Electron Beam Powder Bed Fusion (EB-PBF) as an alternative. EB-PBF runs in vacuum environment and controlled thermal gradients can mitigate postprocessing and encourage the formation of refined microstructures. However, components produced through additive manufacturing (AM) often exhibit anisotropic properties and residual stresses, which must be mitigated through appropriate post-processing. In this work, γ-TiAl bulk rods were fabricated using an EB-PBF system and subsequently subjected to Hot Isostatic Pressing (HIP) and tailored heat treatment strategies to reduce porosity and control microstructural development. Mechanical performance was evaluated through tensile testing at both room and elevated temperatures. This integrated approach aims to overcome key manufacturability limitations while assessing the structural viability of AM-processed γ-TiAl components.

Methodology

TiAl-4822 powder feedstock from Praxair (Danbury, USA) with a particle size distribution of 45–106 μm was used for this study. The powder was produced via vacuum induction melt, argon gas atomization, and had spherical morphology suitable for EB-PBF applications.

Cylindrical rods with a diameter of 15 mm and a height of 76 mm were fabricated as the specimen geometry using an Arcam A2X EB-PBF machine (GE Additive, United States), which features a build envelope of 200 × 200 × 380 mm. A 150 × 150 × 10 mm stainless steel build plate was used, and the EBM control software version was 5.2. The build sequence included outgassing at 700 °C for 10 minutes, followed by powder sintering under the build plate at 1050 °C for 30 minutes. Each layer was deposited with a thickness of 0.070 mm and a hatch distance of 0.20 mm. The preheat was performed using a defocused beam for proper sintering, and the melt was processed with a focused beam for proper melting. The entire process was executed under vacuum. **Table 1** represents process parameters used for part fabrication.

Table 1: Process Parameters for Gamma TiAl Specimen Builds

Stages	Conditions	Parameter
Preheat	Preheat 1	Average Current: 15 mA Repetitions: 5
	Preheat 2	Average Current: 17 mA Repetitions: 8
Melt	Contour Scan	Strategy: Start with the outer contour Passes: 3 (Outer to Inner)
	Hatch Scan	Focus Offset: 4 mA with Speed Function: 50 Current Range: 12 mA – 21 mA

After fabrication, selected samples underwent post-processing via HIP to reduce internal porosity and improve mechanical properties. The HIP treatment was performed using a 6-45H HIP system at 1180 °C for 4 hours under an argon pressure of 200 MPa. Following HIP, two different thermal processing routes were applied as shown in Table 2.

Heat Treatment 1 (HT1) was carried out in-house using a Carbolite Gero tube furnace (Neuhausen, Germany). After initial homogenization above the α-transus temperature (1400 °C), samples were annealed at three different temperatures—1150 °C, 1220 °C, and 1340 °C—for 4 hours each. Furnace cooling was performed at a controlled rate of 5°C/min down to 800°C, followed by a 6-hour aging dwell at 800 °C.

An external thermal processing provider performed Heat Treatment 2 (HT2) due to the specialized equipment required for rapid quenching. Samples were solution-treated at 1220 °C, 1250 °C, or 1280 °C for 4 hours, then gas fan quenched to approximately 700 °C. Subsequently, the temperature increased to 800 °C and was held for 6 hours for aging.

The chosen heat treatment temperatures were based on the Ti-Al phase diagram for a 48% Al composition. HT1 annealing temperatures (1150–1340 °C) span the $\alpha + \gamma$ and α-phase regions with the hope of allowing controlled lamellar refinement and partial homogenization. HT2 solution treatments (1220–1280 °C) were considered to target complete γ-phase dissolution in the α region, followed by aging to re-precipitate a refined lamellar structure.

Table 2: Heat Treatment Protocol Used for Gamma Ti-Al Specimens

Thermal Processing	Temperature	Duration	Cooling Method	Aging Treatment
Heat Treatment 1 (HT1)	1150 °C	4 h	Furnace cooling at 5 °C/min	800 °C, 6 h
	1220 °C	4 h	Furnace cooling at 5 °C/min	800 °C, 6 h
	1340 °C	4 h	Furnace cooling at 5 °C/min	800 °C, 6 h
Heat Treatment 2 (HT2)	1220 °C	4 h	Gas fan quench to ~700 °C, then heat back to 800 °C	800 °C, 6 h
	1250 °C	4 h	Gas fan quench to ~700 °C, then heat back to 800 °C	800 °C, 6 h
	1280 °C	4 h	Gas fan quench to ~700 °C, then heat back to 800 °C	800 °C, 6 h

For metallographic analysis, the samples were sectioned and mounted in black phenolic resin using an ATM OPAL 460 mounting press (Haan, Germany), followed by grinding and polishing using an ATM SAPHIR 530 system. Kroll's reagent was used to etch the polished specimens for microstructural examination. Optical microscopy was employed to inspect the microstructure, and average grain size was measured in accordance with ASTM E112[25].

Mechanical properties were assessed by uniaxial tensile testing. Cylindrical sub-size round specimens conforming to ASTM E8/E8M (gage diameter d = 6 mm, proportional gage length L_0 = 4d = 24 mm; overall length ≈ 70 mm) were machined. Room-temperature tests were conducted according to ASTM E8/E8M on an MTS servo-hydraulic load frame equipped with an MTS 632.24E-50 clip-on extensometer, featuring a 1-inch (25 mm) gage length. Elevated-temperature tests were performed by an external provider in accordance with ASTM E21-20. For both room-temperature and elevated-temperature testing, samples from the HT1 protocol were used because of interest.

Result and Discussion

Microstructure Characterization

Figure 1 presents the etched optical micrographs of the as-built TiAl alloy in the XY (build plane) and Z (build direction) orientations. The microstructure in the XY plane reveals a relatively equiaxed grain morphology with some distribution of spherical pores. In contrast, the Z-plane

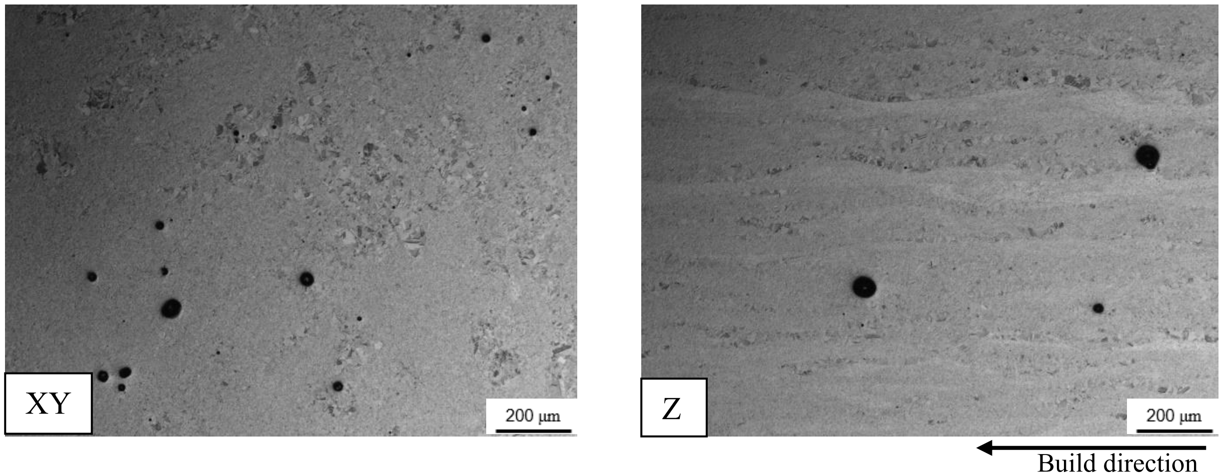

Figure 1 As-built Microstructure of Gamma TiAl Sample in XY and Z Direction (5x magnification ~ 200 microns)

displays elongated grains aligned with the build direction, indicative of directional solidification. Also some pores were also visible in Z-Plane.

Figure 2 shows the microstructure of the post HIP-processed gamma TiAl sample, imaged at 5X and 20X magnifications with the zoomed-in region highlighted. After hot isostatic pressing, the microstructure showed significant densification and homogenization compared to the as built condition. The low magnification image reveals a mostly uniform grain structure with a transition into a coarser grain region, indicating localized grain growth. The high-magnification image shows fine, equiaxed grains with well-defined boundaries and minimal residual porosity. A single, isolated pore remains in the center of the zoomed area. This indicates that although HIP is highly effective at closing internal voids, some porosity can persist.

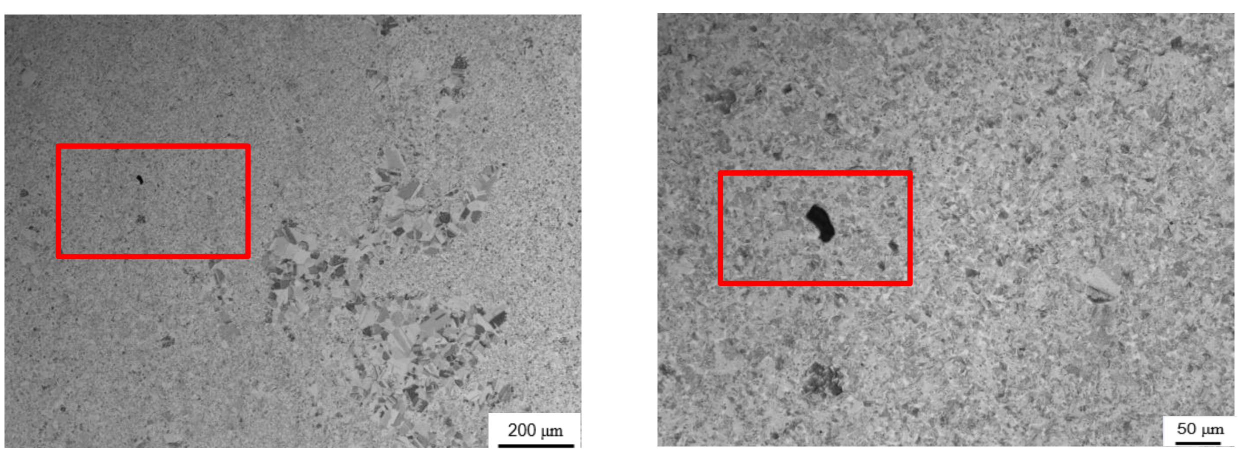

Figure 2 HIPed Microstructure of Gamma TiAl Sample (5x~ 200microns and 20x magnification ~ 50 microns)

Figure 3 shows the microstructure of γ-TiAl samples subjected to the HT1 heat treatment protocol, consisting of annealing at 1150 °C, 1220 °C, and 1340 °C after homogenization, followed by furnace cooling and aging at 800 °C. Images are presented at 5X and 20X magnifications to highlight colony morphology and lamellar evolution.

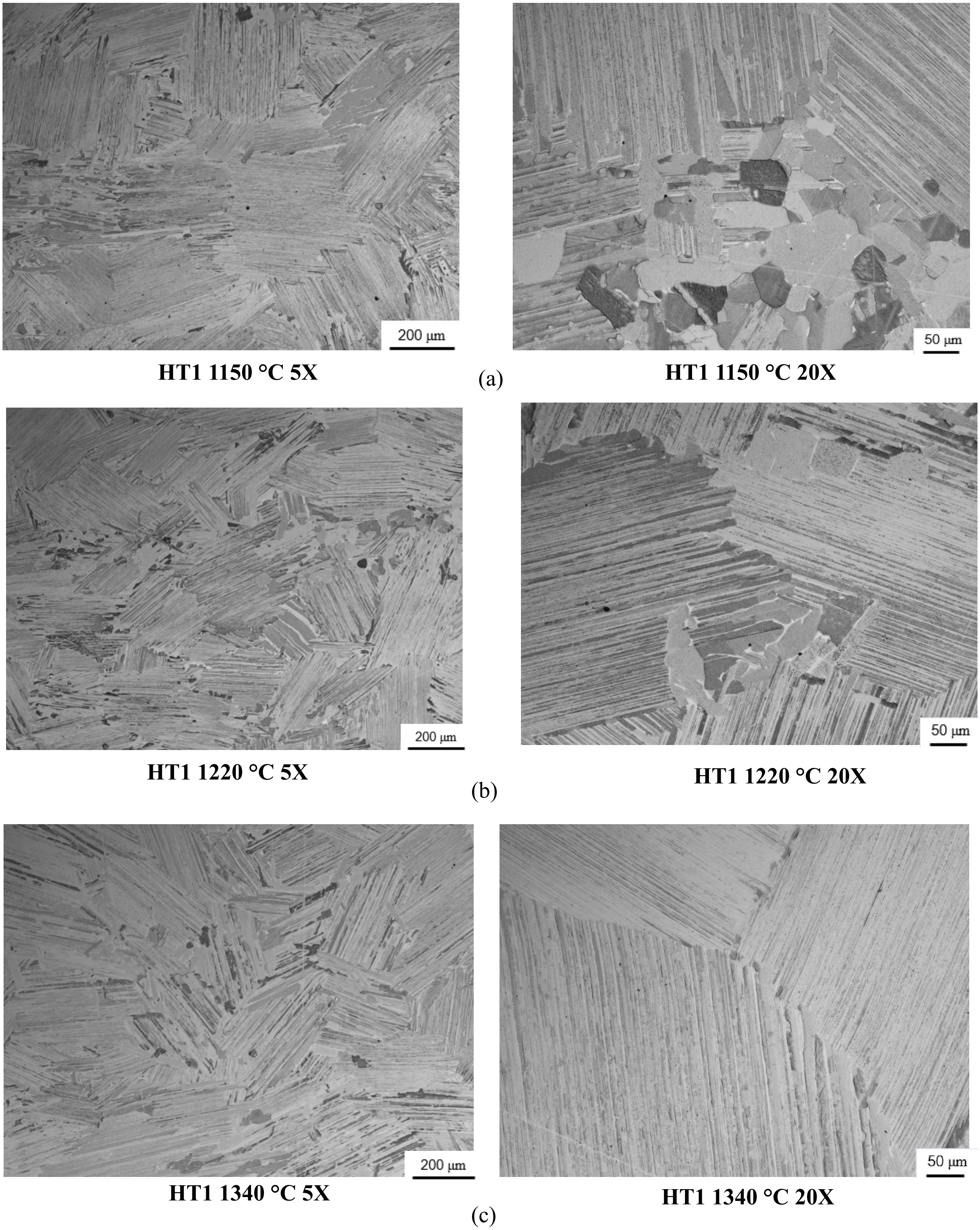

Figure 3 HT1 postprocessed Microstructure of Gamma TiAl Sample (a) 1150 °C (b) 1220 °C and (c) 1340 °C shown at 5x~ 200microns and 20x magnification ~ 50 microns

The microstructure observed at 1150 °C corresponds to the $\alpha + \gamma$ two-phase field. At this temperature, equiaxed γ grains appear with relatively faint etching contrast and coexist with lamellar colonies that are well defined but not yet dominant. This indicates partial transformation of α to a lamellar γ/α_2 structure during slow cooling, resulting in a typical duplex or near-lamellar microstructure.

At 1220 °C, the microstructure transitions toward a more lamellar-dominated morphology. The volume fraction of lamellar colonies increases significantly, with colonies becoming larger, more continuous, and bounded by sharper interfaces. The interlamellar spacing also becomes finer, suggesting deeper penetration into the α phase field during annealing and enhanced γ/α_2 lamellar precipitation upon cooling.

At 1340 °C, the system resides fully within the single-α phase field during annealing. The resulting microstructure consists almost entirely of coarse, well-aligned lamellar colonies with minimal retention of equiaxed γ grains. The colonies exhibit long-range alignment and coarsened lamellae, attributable to increased diffusion rates and extended time above the α-transus. This fully lamellar structure is characteristic of nearly complete α-phase formation followed by γ/α_2 re-precipitation during furnace cooling.

Figure 4 presents the microstructures of γ-TiAl samples subjected to HT2 heat treatment at 1220 °C, 1250 °C, and 1280 °C, followed by gas-fan quench and aging at 800 °C. Samples solution-treated at 1220 °C and 1250 °C exhibit fine-grained, equiaxed γ microstructures with no detectable lamellar colonies. This indicates that the solution treatment did not cross sufficiently into the single-α phase field. As a result, the γ phase remains largely preserved, and subsequent quench inhibits lamellar nucleation. Aging at 800 °C does not initiate significant lamellar transformation, maintaining the fine duplex character.

At 1280 °C, the microstructure reflects partial transformation into the α phase field. Large lamellar colonies become visible, particularly at lower magnifications, yet a substantial fraction of the microstructure remains composed of fine equiaxed γ grains. This mixed morphology suggests incomplete α-phase formation during the solution treatment, potentially due to inadequate soak time or spatial non-uniformity during quench. The presence of both lamellar and equiaxed γ regions is indicative of a transitional structure evolving between the duplex and lamellar regimes.

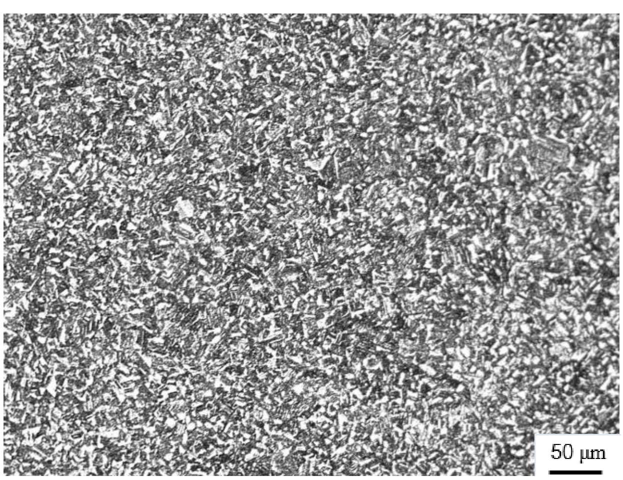

HT2 1220°C 20X

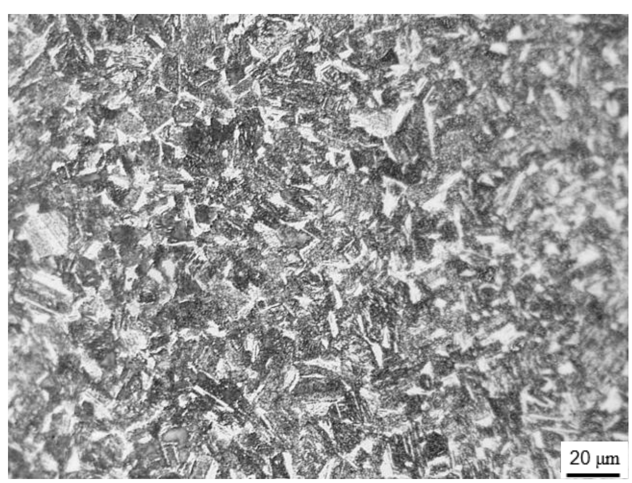

HT2 1220°C 50X

(a)

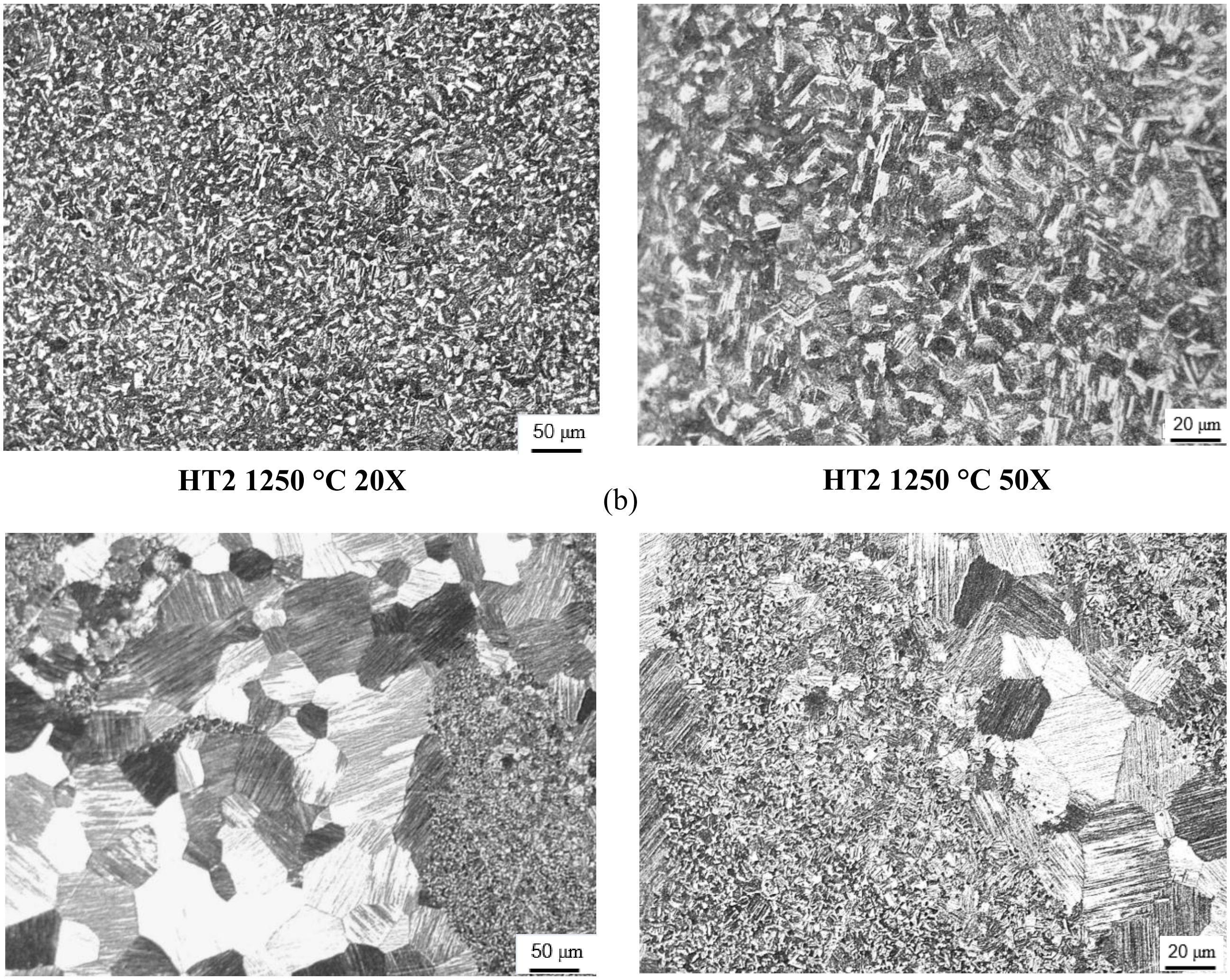

HT2 1250 °C 20X (b) **HT2 1250 °C 50X**

HT2 1280 °C 20X (c) **HT2 1280 °C 50X**

Figure 4 HT2 postprocessed Microstructure of Gamma TiAl Sample (a) 1220 °C (b) 1250 °C and (c) 1280 °C shown at 20x~ 50microns and 50x magnification ~ 20 microns

Tensile Testing

Tensile tests were performed on samples subjected to the HT1 (furnace-cooled) heat treatment specimens. These lamellar microstructure specimens were of particular interest due to their relevance in high-temperature structural applications.

Table 3 presents the yield stress and ultimate tensile strength (UTS) data for the HT1 samples tested at both room temperature and 800 °C, with corresponding strain values summarized. At room temperature, all samples exhibited brittle behavior, with yield strains ranging from 0.004 to 0.005 mm/mm.

Table 3: Results of Room Temperature and High Temperature Tensile Test

Condition	Temperature	Yield Stress (MPa)	Yield Strain (mm/mm)	Ultimate Strength (MPa)
Room Temp	HT1150°C	393	0.005	403
	HT1220°C	364	0.004	420
	HT1340°C	379	0.004	423
High Temp (800°C)	HT1150°C	300	0.008	454
	HT1220°C	289	0.015	468
	HT1340°C	290	0.016	465

The sample annealed at 1150 °C showed the highest yield stress (393 MPa), attributed to its duplex microstructure containing equiaxed γ grains that hinder dislocation motion.

As the annealing temperature increased to 1220 °C and 1340 °C, resulting in more fully lamellar microstructures, the yield stress decreased slightly to 364 MPa and 379 MPa, respectively. However, UTS values increased across this range, reaching 423 MPa at 1340 °C, suggesting that the lamellar colonies offer superior load-bearing capacity once plastic deformation initiates.

At elevated temperature (800 °C), yield stress decreased significantly due to thermally activated deformation mechanisms, but ductility improved. Yield strain values increased from 0.008 mm/mm (HT1150 °C) to 0.016 mm/mm (HT1340 °C), indicating enhanced plasticity in lamellar-rich structures under thermal activation. Notably, UTS values were higher in all high-temperature tests compared to their room-temperature counterparts, with the HT1220 °C sample achieving the highest UTS of 468 MPa. This increase suggests that lamellar microstructures exhibit favorable strength retention and deformability at elevated temperatures.

Conclusion

This study begins with the fabrication of bulk gamma TiAl rods using EB-PBF, followed by HIP and post-processing heat treatments, designated as HT1 and HT2. The HT1 route resulted in lamellar and near-lamellar microstructures due to slow cooling. In contrast, the HT2 samples retained duplex grains with limited lamellar formation due to rapid cooling.

Tensile testing of HT1 specimens revealed brittle behavior at room temperature with yield strains in the range of 0.005 mm/mm, while elevated temperature (800 °C) testing showed improved ductility and strength, mostly aided by thermally activated deformation mechanisms.

These results show that combining EB-PBF with HIP and carefully designed heat treatments can allow for the tailoring of microstructure and improve the mechanical performance of gamma TiAl bulk rods. This further makes them well-suited for demanding aerospace and high-temperature applications.

Acknowledgements

This research was conducted at the W.M. Keck Center for 3D Innovation at The University of Texas at El Paso (UTEP). The authors thank Aldo Rubio Hidalgo and Alex De la Cruz for their assistance with machine setup, and Dana Godinez for metallography and imaging support. We also acknowledge Ron Aman and Bill Mohr from EWI for their technical guidance. Funding was provided by the UTEP Keck Center and the Mr. and Mrs. MacIntosh Murchison Chair I in Engineering Endowment. Special thanks go to Chad Beamer (Quintus Technologies) for his support with the HIP process and to Brian Baughman (Honeywell Aerospace) for his technical collaboration on the heat treatment process.

References

[1] O. Genc and R. Unal, "Development of gamma titanium aluminide (γ-TiAl) alloys: A review," *Journal of Alloys and Compounds*, vol. 929, p. 167262, Dec. 2022, doi: 10.1016/j.jallcom.2022.167262.

[2] S. T. Nabil *et al.*, "Microstructure Refinement of Bulk Inconel 718 Parts During Fabrication with EB-PBF Using Scanning Strategies: Transition from Bidirectional-Raster to Stochastic Point-Based Melting," *Journal of Manufacturing and Materials Processing*, vol. 8, no. 6, p. 241, Dec. 2024, doi: 10.3390/jmmp8060241.

[3] J. C. Diaz *et al.*, "Effect of Layer Thickness and Heat Treatment on Microstructure and Mechanical Properties of Alloy 625 Manufactured by Electron Beam Powder Bed Fusion," *Materials*, vol. 15, no. 21, Art. no. 21, Jan. 2022, doi: 10.3390/ma15217767.

[4] S. Huang, Y.-C. Lin, and R.-J. Chung, "A Review of the State of Art of Fabrication Technologies of Titanium Aluminide (Ti-Al) Based on US Patents," *Metals*, vol. 14, no. 4, Art. no. 4, Apr. 2024, doi: 10.3390/met14040418.

[5] S. T. Nabil *et al.*, "Effect of Two Different Point-Based Melt Scanning Strategies on the Microstructure of As-Built IN718 Parts Fabricated via EB-PBF System," 2024, Accessed: Sep. 21, 2025. [Online]. Available: https://doi.org/10.26153/tsw/58107

[6] "TiAl alloys in commercial aircraft engines: Materials at High Temperatures: Vol 33, No 4-5." Accessed: Jun. 24, 2025. [Online]. Available: https://www.tandfonline.com/doi/abs/10.1080/09603409.2016.1183068

[7] "Development of the GE Aviation Low Emissions TAPS Combustor for Next Generation Aircraft Engines," Aerospace Sciences Meetings. Accessed: Jun. 24, 2025. [Online]. Available: https://arc.aiaa.org/doi/10.2514/6.2012-936

[8] K. I. Watanabe, "Electron Beam Melted Parameter Development Of Pure Tungsten & Post-Processing Hip And Heat Treatment Of Gamma Titanium Aluminide".

[9] S. L. Draper *et al.*, "Development and evaluation of TiAl sheet structures for hypersonic applications," *Materials Science and Engineering: A*, vol. 464, no. 1, pp. 330–342, Aug. 2007, doi: 10.1016/j.msea.2007.02.020.

[10] B. Dimčić, M. T. Jovanović, I. Bobić, S. Zec, and S. Tadić, "TiAl – A New High Temperature Material for Turbocharger Rotors," *Materials Science Forum*, vol. 453–454, pp. 169–174, 2004, doi: 10.4028/www.scientific.net/MSF.453-454.169.

[11] S. A. Raji, A. P. I. Popoola, S. L. Pityana, and O. M. Popoola, "Characteristic effects of alloying elements on β solidifying titanium aluminides: A review," *Heliyon*, vol. 6, no. 7, p. e04463, Jul. 2020, doi: 10.1016/j.heliyon.2020.e04463.

[12] B. Ramirez *et al.*, “Effects of Process Parameters and Process Defects on the Flexural Fatigue Life of Ti-6Al-4V Fabricated by Laser Powder Bed Fusion,” *Materials*, vol. 17, no. 18, Art. no. 18, Jan. 2024, doi: 10.3390/ma17184548.

[13] W. Chen and Z. Li, “11 - Additive manufacturing of titanium aluminides,” in *Additive Manufacturing for the Aerospace Industry*, F. Froes and R. Boyer, Eds., Elsevier, 2019, pp. 235–263. doi: 10.1016/B978-0-12-814062-8.00013-3.

[14] F. H. Froes, C. Suryanarayana, and D. Eliezer, “Synthesis, properties and applications of titanium aluminides,” *J Mater Sci*, vol. 27, no. 19, pp. 5113–5140, Oct. 1992, doi: 10.1007/BF02403806.

[15] T. C. Dzogbewu and W. B. du Preez, “Additive Manufacturing of Ti-Based Intermetallic Alloys: A Review and Conceptualization of a Next-Generation Machine,” *Materials*, vol. 14, no. 15, Art. no. 15, Jan. 2021, doi: 10.3390/ma14154317.

[16] S. A. Raji, A. P. I. Popoola, S. L. Pityana, and O. M. Popoola, “Characteristic effects of alloying elements on β solidifying titanium aluminides: A review,” *Heliyon*, vol. 6, no. 7, p. e04463, Jul. 2020, doi: 10.1016/j.heliyon.2020.e04463.

[17] D. Laurin, D. Seo, H. Saari, and Y. W. Kim, “The Effects of Hot Isostatic Pressing Conditions on the Microstructure of Beta-Gamma Titanium Aluminide Powder Alloys,” *Advanced Materials Research*, vol. 89–91, pp. 325–330, 2010, doi: 10.4028/www.scientific.net/AMR.89-91.325.

[18] “Microstructure Design and Its Effect on Mechanical Properties in Gamma Titanium Aluminides.” Accessed: Jun. 24, 2025. [Online]. Available: https://www.mdpi.com/2075-4701/11/10/1644

[19] R. Hood, “The machinability of a gamma titanium aluminide intermetallic,” d_ph, University of Birmingham, 2010. Accessed: Jun. 24, 2025. [Online]. Available: https://etheses.bham.ac.uk/id/eprint/1380/

[20] I. Polozov, V. Sokolova, A. Gracheva, and A. Popovich, “Tailoring the Microstructure of Laser-Additive-Manufactured Titanium Aluminide Alloys via In Situ Alloying and Parameter Variation,” *Metals*, vol. 13, no. 8, Art. no. 8, Aug. 2023, doi: 10.3390/met13081429.

[21] C. Banuelos *et al.*, “Fatigue Endurance Investigation of Post-processed Surfaces of LPBF Ti-6Al-4V under Flexural Stress,” University of Texas at Austin, 2023. Accessed: Jul. 01, 2024. [Online]. Available: https://doi.org/10.26153/tsw/51092

[22] R. Yang, Y. Y. Cui, L. M. Dong, and Q. Jia, “Alloy development and shell mould casting of gamma TiAl,” *Journal of Materials Processing Technology*, vol. 135, no. 2, pp. 179–188, Apr. 2003, doi: 10.1016/S0924-0136(02)00873-7.

[23] G. Ge, Z. Wang, S. Liang, and L. Zhang, “Achievement of forging without canning for β-solidifying γ-TiAl alloy containing high content of niobium,” *Materials and Manufacturing Processes*, Oct. 2021, Accessed: Jun. 24, 2025. [Online]. Available: https://www.tandfonline.com/doi/abs/10.1080/10426914.2021.1942902

[24] A. S. Ramos, M.-T. F. Vieira, M. F. Vieira, and F. Viana, “Joining of Gamma-Based Titanium Aluminides – A Review,” *Materials Science Forum*, vol. 514–516, pp. 483–489, 2006, doi: 10.4028/www.scientific.net/MSF.514-516.483.

[25] “Standard Test Methods for Determining Average Grain Size.” Accessed: Jun. 24, 2025. [Online]. Available: https://store.astm.org/e0112-13r21.html